View metadata, citation and similar papers at core.ac.uk
brought to you by CORE
provided by National Chung Hsing University Institutional Repository

Journal of The Electrochemical Society, **160** (9) H581-H586 (2013)
0013-4651/2013/160(9)/H581/6/$31.00 © The Electrochemical Society

Surface Metallization of Polyimide as a Photoanode Substrate for Rear-Illuminated Dye-Sensitized Solar Cells

Yu-Ting Huang,[a,b] Ya-Yun Zhan,[a] Sheng-Jye Cherng,[a] Chih-Ming Chen,[a,z] Shien-Ping Feng,[b] and Tzu-Chien Wei[c]

[a]*Department of Chemical Engineering, National Chung Hsing University, Taichung 402, Taiwan*
[b]*Department of Mechanical Engineering, The University of Hong Kong, Hong Kong*
[c]*Department of Chemical Engineering, National Tsing-Hua University, Hsinchu 300, Taiwan*

Plastic film is promising as a photoanode substrate of dye-sensitized solar cell (DSSC) for flexible applications, while a low-temperature sintering process is generally adopted for the TiO_2 mesoporous film due to unstable thermal property of general plastics. This study demonstrates that typical high-temperature TiO_2 sintering can be adopted for preparing the photoanode when using a surface-metallized polyimide (PI) film. A Sn/Ni bi-layer is formed on a PI film via a chemical process as the conductive layer. The Sn/Ni-coated PI photoanode can withstand high-temperature TiO_2 sintering at a peak temperature of 430°C for 30 min without significant visual deformation due to high thermal stability of PI and strength reinforcement caused by surface metallization. The DSSC employing the Sn/Ni-coated PI film as the photoanode substrate reaches an energy conversion efficiency of 3.44% under 1 sun rear-side illumination.
© 2013 The Electrochemical Society. [DOI: 10.1149/2.046309jes] All rights reserved.

Manuscript submitted April 30, 2013; revised manuscript received May 30, 2013. Published June 25, 2013.

Development of stable and abundant alternative energy continues to be an important issue for human society because of inevitable shortage of fossil fuel in the future. Solar energy fits most of the requirements as a promising alternative energy and therefore attracts much attention in the past half century. How to effectively utilize solar energy and to convert it into electricity strongly depends upon performance of photovoltaic devices. Until now, Si-based solar cells invented by Bell laboratory in 1954[1] have been developed as one of the most successful photovoltaic devices and have been commercially applied. However, Si-based solar cells are not widely popularized yet in human daily life due to high cost resulted from expensive fabrication procedure and equipment. Cost down is still an important task for popularization of Si-based solar cells.

In 1991, a low-cost, high-efficiency solar cell based on dye-sensitized mesoporous TiO_2 film, named as dye-sensitized solar cell (DSSC), was proposed as a new type of photovoltaic device.[2] Due to easy and cost-efficient fabrication, DSSC quickly attracts attention and numerous efforts are devoted to make it possible in real commercialization.[3,4] A typical DSSC consists of three major components: a dye-adsorbed TiO_2 mesoporous film coated on a transparent conductive oxide (TCO) glass as the photoanode, an electrolyte system containing iodide/tri-iodide (I^-/I_3^-) redox couple in a proper mediator, and a counter electrode capable to catalyze the tri-iodide reduction. The energy conversion efficiency of DSSC has reached above 12%[5] when employing zinc-porphyrin dye with cobalt-based electrolyte, which is a great progress for real commercialization.

Conventional DSSCs employ fluorine-doped SnO_2 (FTO) transparent conduction glass as the photoanode substrate due to its good conductivity and thermal stability. However, the FTO glass substrates are rigid and lack shape-modified flexibility, which makes DSSC unsuitable for flexible and lightweight applications. In order to broaden DSSC's application, efforts have been made to investigate the feasibility of flexible substrates as the cell electrode.[6–16] The employment of flexible substrates can also make roll-to-roll production possible for DSSCs.

Metallic foils, including titanium, stainless steel, and nickel, are promising candidates as flexible electrode substrate for DSSCs.[6–14,16] The major characteristic of metallic substrates is their superior electrical conduction property which is beneficial for electron transfer in the DSSC operation. However, metals still need to meet some requirements, like high stability in the corrosive liquid electrolytes and suitable energy level arrangement between surface oxide layer and TiO_2 mesoporous film. In addition to metallic substrates, plastic films are also promising as flexible electrode substrates.[13,15,17–24] Polyethylene terephthalate (PET) and polyethylene naphthalate (PEN) coated with tin-doped indium oxide (ITO) are proposed as the photoanode substrate due to their high transparency. However, to overcome temperature-sensitive disadvantage of general plastic materials, a low-temperature treatment of TiO_2 mesoporous film at roughly 150°C is usually employed[17–23] instead of typical high-temperature sintering at above 450°C. Low-temperature sintering inevitably degrades the connection among TiO_2 nanoparticles and adherence between electrode and TiO_2 mesoporous film.

In this study, we demonstrated that polyimide (PI) could be used as the photoanode substrate for DSSC without significantly lowering the sintering temperature of TiO_2 mesoporous film. Compared with PET and PEN, PI generally possesses a higher glass transition temperature. Such high thermal stability enables PI to withstand high sintering temperature. In addition, PI has good mechanical strength and superior chemical resistance in acidic environments[25] which are beneficial for practical application. The primary disadvantage of PI is its lower transparency, so the DSSC employing PI as the photoanode substrate is suggested to be rear-illuminated. To make PI conductive, the PI surface was modified first[26] and then a Ni layer was chemically deposited on the modified PI surface[15] as a conductive layer. The reason of using Ni is due to its high stability against the corrosive electrolyte.[13] The Ni-coated PI film had been demonstrated as an efficient substrate of counter electrode for DSSC,[15] while to the best of our knowledge, this study was for the first time to employ the Ni-coated PI film as the photoanode substrate for DSSC. As mentioned above, we considered that high thermal stability of PI enabled itself to be another promising candidate as the plastic photoanode substrate besides common PET and PEN films. A Sn layer was further deposited on the Ni-coated PI film using electroplating to produce a SnO_2 layer to meet the energy level arrangement with the TiO_2 mesoporous film.[16] In comparison with the previous study employing a single Ni foil as the photoanode substrate,[16] a Ni/PI composite substrate is more attractive for lightweight applications. For plastic substrates used in DSSC, sputtering is a method commonly used to deposit a conductive ITO layer on PET and PEN films. By contrast, surface metallization of PI film in this study was carried out by a chemical process, which provided a more economic method to prepare a conductive plastic substrate. The DSSC employing the Sn/Ni-coated PI film as the photoanode substrate achieved an energy conversion efficiency of 3.44% under 1 sun rear-side illumination.

Experimental

Preparation of plastic photoanode and fabrication of DSSC.— A piece of PI film (2 × 3 cm^2) was cut from commercially purchased

[z]E-mail: chencm@nchu.edu.tw

Downloaded on 2013-11-18 to IP 140.120.136.205 address. Redistribution subject to ECS license or copyright; see ecsdl.org/site/terms_use

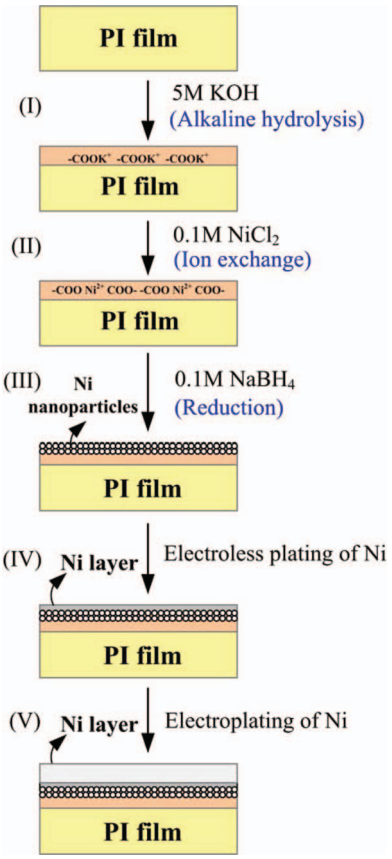

Figure 1. Chemical treatment process for surface metallization of PI film.

sample (DuPont, 125 μm thick, glass transition temperature (T_g) = 360°C ~ 410°C depending upon different measurement techniques) and was cleaned ultrasonically in ethanol and deionized water, respectively, for 15 min to remove surface contamination. Then, surface metallization of PI film was carried out following a chemical process shown in Fig. 1 and the details was described elsewhere.[15] First, the PI film was immersed into a 5 M KOH solution (Sigma-Aldrich) at room temperature for 1 min for surface modification, after which an potassium salts of poly(amic acid) layer (PAA) was formed on the PI surface.[26] The PI film was then immersed into a 0.1 M $NiCl_2$ solution (Allied Signal) at room temperature for 1 min to dope Ni^{2+} ions into the sublayer via an ion exchange reaction. The doped Ni^{2+} ions were reduced to Ni nanoparticles using 0.1 M $NaBH_4$ (Sigma-Aldrich) as the reductant. The Ni nanoparticles inserted on the PI surface functioned as seeds to trigger subsequent electroless deposition of Ni atoms at 85°C for 3 min[27] using Ni_2SO_4 as the electrolyte (Atotech, Taiwan). To thicken the Ni layer as a conductive and mechanically strong layer, electroplating was performed at 45°C for 5 min using a Ni-based electrolyte purchased from local industry (Sheng Hung Chemical Engineering CO., LTD, Taiwan). The plating current density was controlled at 0.33 A/cm^2. The Ni layer was thickened to 12-13 μm after electroplating. The above-mentioned chemical process was performed on only one side of the PI film.

A Sn layer was grown on the Ni-coated PI film using electroplating ($SnSO_4$, Atotech, Taiwan) at 10°C. The plating current density was controlled at 0.02, 0.1, and 0.5 A/cm^2 and plating time varied from 10 to 480 s. Table I lists the electroplating parameters used in this study. After Sn electroplating, a TiO_2 mesoporous film (Ti-Nanoxide T20/SP, Solaronix) of 12–14 μm thickness was screen-printed on the Sn surface. The screen-printing area of the TiO_2 film was 0.16 cm^2. The TiO_2-coated PI film was heated in a furnace. The peak temperature of the heating profile was set at 430°C and the duration was 30 min. It needed to mention that we tried several peak temperatures for the TiO_2 sintering process and suggested that 430°C was the optimized one because beyond which significant visual deformation was observed for the PI film. Though 430°C was a little higher than the value of T_g of PI (360°C ~ 410°C), no visual deformation was observed for the Sn/Ni-coated PI film after high-temperature sintering. This could be attributed to strength reinforcement of the PI film after surface metallization. After TiO_2 sintering, the PI-based photoanode was then immersed in a 0.4 mM N719 dye solution (Solaronix) at room temperature for 12 h to allow dye adsorption onto the TiO_2 nanoparticles, followed by rinsing with ethanol and drying in air.

A 1.5 × 2 cm^2 ITO glass sheet (7Ω/□, 1.1 mm thick, Gem Tech.) was cleaned in 4 wt% detergent in an ultrasonic bath for 15 min, followed by rinsing with de-ionized water. Platinum was deposited on the ITO glass sheet using sputtering at 20 mA for 20 s as the counter electrode. The thickness of the sputtered Pt layer was only 2 nm, so the ITO glass sheet remained highly transparent and was suitable for DSSC operation under rear-side illumination.[16] The dye-adsorbed TiO_2 photoanode and the Pt-coated counter electrode were stacked face-to-face and sealed with a 25-μm-thick thermal-plastic Surlyn spacer (SX1170-25, Solaronix). A proper amount of liquid electrolyte (0.2 M PMII, 0.05 M I_2, 0.1 M LiI, 0.2 M TBAI, 0.5 M TBP in AN/VN, AN:VN = 85:15) was injected into the gap between two electrodes. The configuration of as-assembled DSSC is schematically shown in Fig. 2.

Measurements and characterizations.— The fabricated DSSC was evaluated under AM 1.5 (1 sun, 100 mW/cm^2) rear-side illumination with a solar simulator (YSS-E40, Yamashita Denso Corp., Japan). Photocurrent-voltage (*J-V*) curves were recorded using a computer-controlled digital source meter (Keithley, model 2400). The electron transport property, such as lifetime, in DSSCs was measured

Table I. Electroplating parameters for Sn deposition on the Ni-coated PI film and photovoltaic parameters of DSSCs employing Sn/Ni-coated PI photoanode under rear-side illumination.

Type	Current density for Sn electroplating (A/cm^2)	Plating time (sec)	V_{OC} (V)	J_{SC} (mA/cm^2)	FF	η (%)	τ_n (ms)
Ni/PI	–	–	0.690	3.236	0.188	0.425	–
ITO/PI	–	–	0.682	6.542	0.541	2.415	–
A-1		240	0.673	7.036	0.692	3.282	20.46
A-2	0.02	360	0.691	6.651	0.697	3.201	19.55
A-3		480	0.664	7.013	0.629	2.914	18.97
B-1		50	0.701	7.264	0.645	3.272	20.88
B-2	0.1	75	0.707	6.630	0.667	3.129	20.56
B-3		100	0.695	6.81	0.626	2.979	18.84
C-1		10	0.681	7.025	0.72	3.44	21.89
C-2	0.5	15	0.666	7.408	0.684	3.373	20.73
C-3		20	0.652	7.543	0.65	3.193	14.35

Downloaded on 2013-11-18 to IP 140.120.136.205 address. Redistribution subject to ECS license or copyright; see ecsdl.org/site/terms_use

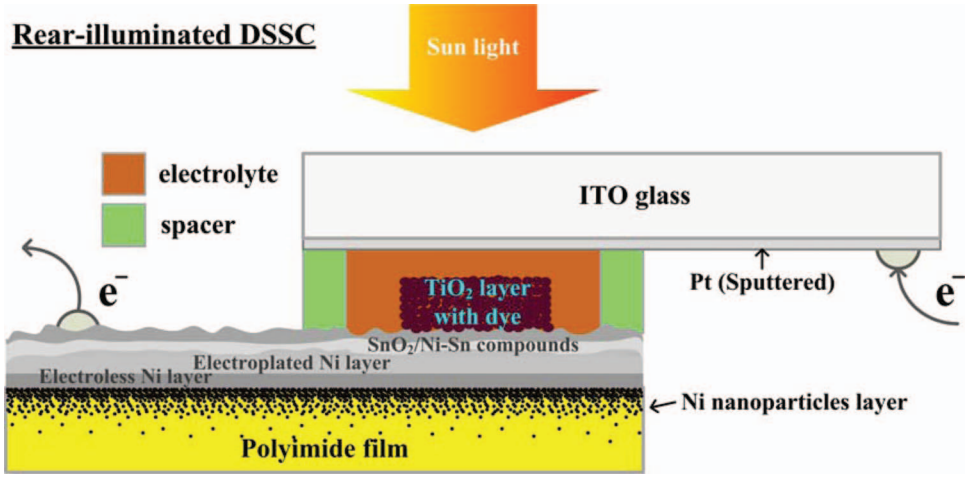

Figure 2. Schematic diagram of the configuration of DSSC based on PI photoanode.

using intensity modulated photocurrent spectroscopy (IMPS) and intensity modulated photovoltage spectroscopy (IMVS) equipped with a potentiostat/galvanostat (PGSTAT 302N, Autolab, Eco-Chemie, Netherlands).[28] A light-emitting diode with a light intensity up to 6.36 mW/cm^2 on electrodes was used as the light source. The frequency range was 10 kHz to 1 Hz.

The surface morphology of the PI film after surface modification and chemical treatment was also examined using a scanning electron microscope (SEM, JEOL, Japan). SEM was also used to observe the surface morphology of the as-plated Sn layer on the Ni-coated PI film. The Sn/Ni-coated PI film was also cross-sectioned to expose the Ni/PI and Sn/Ni interfaces for SEM and optical microscope (OM) observation. Compositional analysis of any new phase formed at the Sn/Ni interface was carried out using an energy dispersive X-ray spectrometer (EDX).

Results and Discussion

Surface examination of the PI film after surface modification and chemical treatment.— Before any surface treatment, the bare PI film exhibited a flat surface morphology as shown in Fig. 3a. After KOH treatment for 1 min, as shown in Fig. 3b, no significant change was observed on the PI surface. The PI surface still remained a flat morphology after $NiCl_2$ ion exchange, as seen in Fig. 3c. After $NaBH_4$ reduction, a significant morphological change was observed on the PI surface. As seen in Fig. 3d, high-density of Ni nanoparticles were formed on the PI surface. Their diameter was about 10 nm. These Ni nanoparticles were used as seeds for subsequent electroless plating. It could be found that the particle distribution was quite uniform and such high uniformity was beneficial for electroless plating. Fig. 3e shows that dense and granular Ni particles were formed on the PI surface after electroless deposition of Ni.

Surface examination of the PI film after electroplating of Sn at various current densities.— Fig. 4 shows the surface morphologies of as-plated Sn layers on the Ni-coated PI film under various current densities. It was found that the surface morphologies of as-plated Sn layers were quite different for various current densities. For the current density of 0.02 A/cm^2, as seen in Fig. 4a–4c, faceted-shaped Sn grains were formed and stacked densely on the Ni-coated PI film. When the current density was increased to 0.1 A/cm^2, as seen in Fig. 4d–4f, the Sn grains formed were also faceted-shaped but their average size was much smaller than those in Fig. 4a–4c. In other words, the grain quantity within a specific area, i.e. grain density, increased with increasing the current density. This could be attributed to enhanced nucleation rate caused by the increase of current density. When the current density was increased to 0.5 A/cm^2, the deposition rate of Sn atoms was also enhanced, making the Sn grains grow at a faster rate and some of them agglomerated to form bigger grains as seen in Fig. 4g–4i. Rapid deposition of Sn atoms also led to isotropic-like growth of the Sn grains, so the Sn grains were formed in the form of granules.

Cross-sectional examination of the PI film after surface metallization.— Fig. 5a shows the SEM image of the cross section of the PI film after chemical treatment as illustrated in Fig. 1. It was found that a tri-layer structure was formed on the PI film. The bottom layer, i.e. just above the PI film, was formed after $NaBH_4$ reduction and was about 3 μm thick. The $NaBH_4$ treatment reduced the doped Ni^{2+} ions to Ni atoms and the reduced Ni atoms agglomerated to form nanoparticles inserted into the sublayer of the PI film. So, it could be

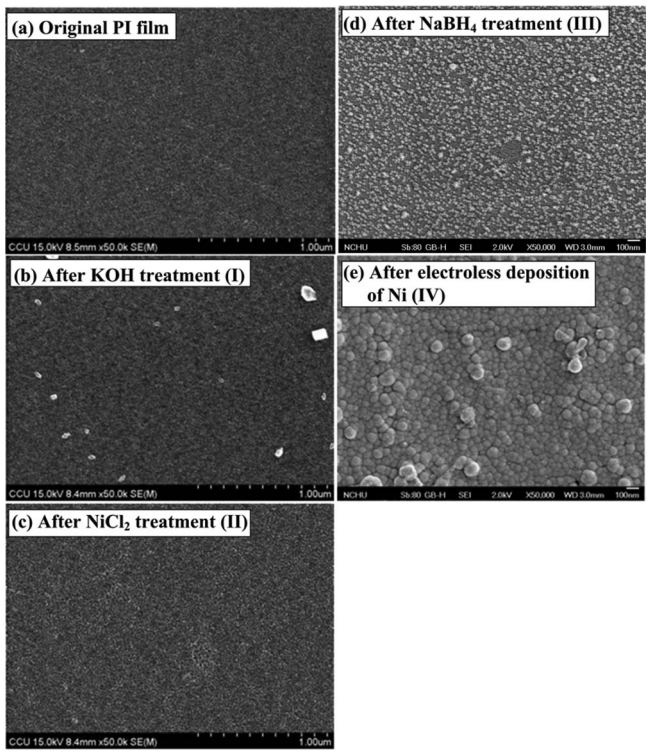

Figure 3. SEM images showing the surface morphologies of the PI film after chemical treatment illustrated in Fig. 1.

Downloaded on 2013-11-18 to IP 140.120.136.205 address. Redistribution subject to ECS license or copyright; see ecsdl.org/site/terms_use

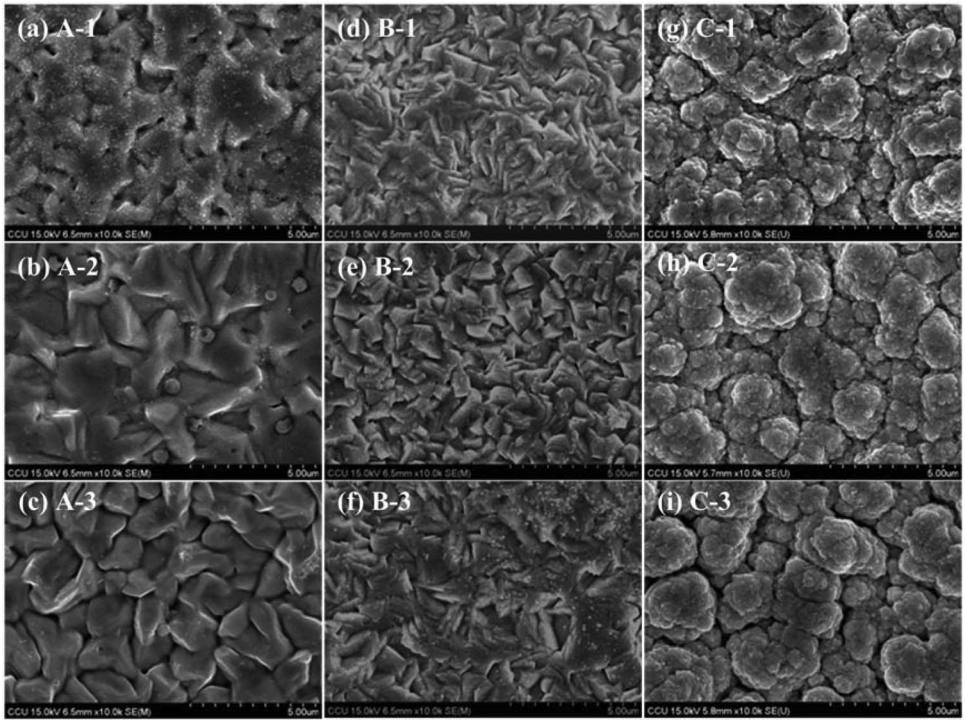

Figure 4. SEM images showing the surface morphologies of as-plated Sn layers on the Ni-coated PI film under various current densities: (a)-(c) 0.02 A/cm^2, (d)-(f) 0.1 A/cm^2, (g)-(i) 0.5 A/cm^2.

found that this layer was composed of high density of Ni nanoparticles. The second layer was formed after electroless deposition of Ni and its thickness was about 1 μm. Since electroless deposition was difficult to form a thick and compact metallic layer, electroplating was used to form a 13-μm-thick Ni layer as the top layer. The electroplated Ni layer could significantly improve the electrical conduction capability of the PI film. The mechanical strength of the PI film could also be enhanced which enabled itself to withstand high-temperature TiO_2 sintering. The sample in Fig. 5a was further treated by electroplating of Sn and high-temperature treatment at 430°C for 30 min. As seen in Fig. 5b, no significant degradation and alteration was observed for the PI film after high-temperature treatment. An inset photo also indicated the Sn/Ni-coated PI film after high-temperature treatment was still flexible. Therefore, we considered that the Sn/Ni-coated PI film after a 30 min, 430°C sintering process was still workable for DSSC. Fig. 5c shows an enlarged SEM image of the marked region (dotted rectangle) in Fig. 5b. It was found that two intermetallic compounds, top Ni_3Sn_4 and bottom Ni_3Sn_2, were formed on the electroplated Ni layer. It indicated that the electroplated Sn layer was completely consumed by the Sn/Ni interfacial reaction during high-temperature treatment and was transformed into the intermetallic compounds. As reported previously,[16] a SnO_2 layer was also formed on top of the intermetallic compounds after high-temperature treatment. Formation of the intermetallic compounds and a Sn-based oxide layer were beneficial for DSSC operation and were discussed in the next section.[16]

Photovoltaic characteristics of DSSCs based on surface-metallized PI photoanodes.— Fig. 6 shows the photocurrent-voltage (*J-V*) curves of the DSSCs based on various types of PI-based photoanodes. From Fig. 6, the photovoltaic parameters of the DSSCs can be deduced and are listed in Table I. It has to note that the *J-V* curves shown in Fig. 6 stand for some representative cells (i.e. each curve stands for a single cell), while the data listed in Table I are an average of at least five samples. As seen, the DSSC employing Ni-coated PI film (without Sn deposition) as the photoanode substrate exhibited a very low efficiency ($\eta = 0.425\%$). As discussed previously,[16] a p-type NiO layer may be formed on the Ni surface after high-temperature sintering of TiO_2 mesoporous film. This p-type layer was unfavorable for electron transfer from n-type TiO_2 mesoporous film to the photoanode. So, the cell efficiency was worse. When a Sn layer was deposited on the Ni-coated PI film as the photoanode substrate, the photovoltaic performance of resultant DSSCs was significantly improved as seen in Table I. Such improvement of photovoltaic performance was attributed to formation of a bi-layer of SnO_2 and Ni-Sn intermetallic compounds between the TiO_2 mesoporous film and Ni-coated PI film after high-temperature TiO_2 sintering.[16] The top n-type SnO_2 layer enabled electron transfer from the TiO_2 mesoporous film to the Ni-coated PI film because of appropriate energy level arrangement between SnO_2 and TiO_2. The interfacial Ni-Sn intermetallic compounds were beneficial for electron transfer because they were good electrical conductors. In Table I, it was found that the energy conversion efficiency (η) of DSSC approximately decreased with increasing the plating time for all current densities. In general, longer the plating time, thicker the electroplated Sn layer. In other words, the DSSC's performance got worse when the electroplated Sn layer became thicker. During high-temperature TiO_2 sintering, a SnO_2 layer would be formed on top of the Sn layer.[16] In addition, the Sn layer would melt and react with underlying Ni to form Ni-Sn intermetallic compounds. The formation of solid Ni-Sn intermetallic compounds was more advantageous for supporting the TiO_2 mesoporous film in comparison with a molten Sn layer because molten Sn was mechanically weak. Weak supporting was likely to destroy the top SnO_2 layer as well as the adhesion between the Sn layer and the TiO_2 mesoporous film. Therefore, a thicker Sn layer should be avoided because it would take much longer for complete phase transformation from molten Sn to solid Ni-Sn intermetallic compounds. This was why the DSSC's performance got worse with increasing the thickness of electroplated Sn layer. Dark current experiments, as seen in Fig. 7, also showed a similar trend. The dark current was found to increase with increasing the plating time (i.e. the Sn layer thickness). As mentioned above, adhesion between the Sn layer and the TiO_2 mesoporous film became unstable when the thickness of the Sn layer increased. Unstable adhesion would hinder electron transfer or create defect sites as electron traps, so back reaction (charge recombination) was enhanced as well as the dark current. The electron lifetime listed

Downloaded on 2013-11-18 to IP 140.120.136.205 address. Redistribution subject to ECS license or copyright; see ecsdl.org/site/terms_use

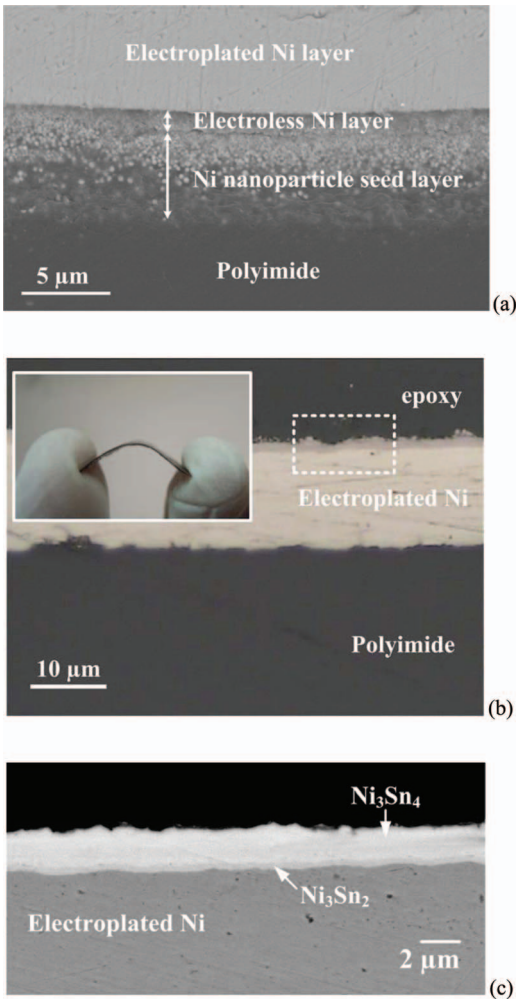

Figure 5. (a) SEM image of the cross section of the PI film after chemical treatment as illustrated in Fig. 1 (i.e. after Ni electroplating). (b) OM micrograph of the cross section of the Ni-coated PI film after electroplating of Sn and high-temperature treatment at 430°C for 30 min, where the inset showed that the Sn/Ni-coated PI film after high-temperature treatment was still flexible. (c) Enlarged SEM image of the marked region (dotted rectangle) in (b).

in Table I also showed that thicker the Sn layer, shorter the electron lifetime, which was consistent with the results of dark current.

We also used ITO-coated PI film as the photoanode substrate for DSSC, where the ITO layer was 200 nm and was deposited on the PI film using sputtering. From Table I, the DSSC based on ITO-coated PI film exhibited an efficiency of about 2.4%, which was lower than those based on Sn/Ni-coated PI film. This indicated that surface-metallized PI film was a promising candidate as the photoanode substrate for DSSC under rear-side illumination. In comparison with the ITO coating using sputtering, surface metallization of PI was carried out by a chemical process, which was more cost-efficient for mass production.

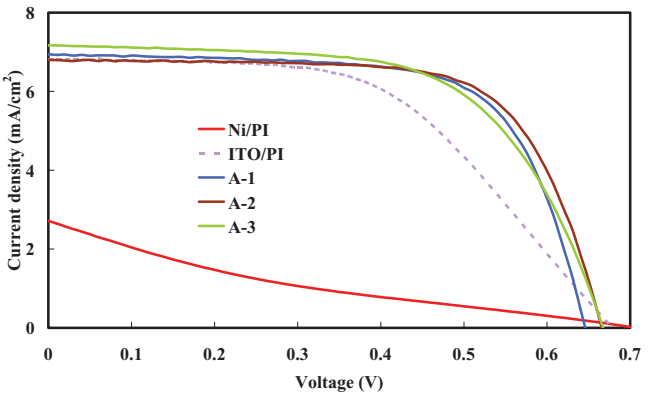

Figure 6. Photocurrent-voltage (*J*-*V*) curves of the DSSCs based on various types of PI-based photoanode substrates.

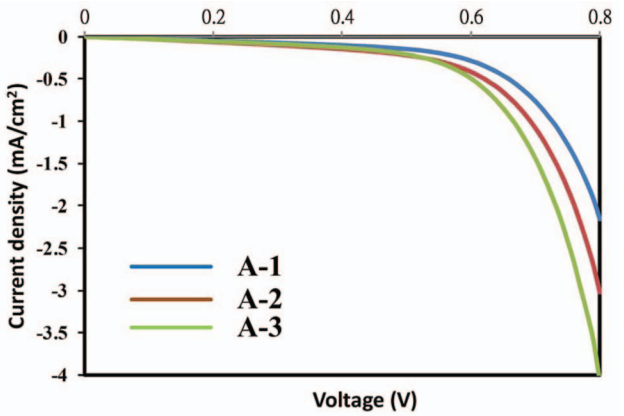

Figure 7. Photocurrent-voltage (*J*-*V*) curves of the DSSCs under dark condition.

Conclusions

Polyimide becomes electrically conductive after surface metallization of a Sn/Ni bi-layer and is successfully employed as a photoanode substrate for DSSC. The major advantage of polyimide in the DSSC application is its relatively high glass transition temperature in comparison with general plastics. Such high thermal stability and reinforcement of mechanical strength by surface metallization enable the PI-based photoanode to withstand high-temperature sintering of TiO_2 mesoporous film at a peak temperature of 430°C for 30 min without significant visual deformation. The DSSCs based on the PI-based photoanodes exhibit good energy conversion efficiency with an average value above 3%, and the peak efficiency of 3.44% can be achieved by optimizing the plating parameters of the Sn/Ni bi-layer.

Acknowledgments

The authors thank the financial support of the National Science Council, Taiwan, ROC.

References

1. D. M. Chapin, C. S. Fuller, and G. L. Pearson, *J. Appl. Phys.*, **25**, 676 (1954).
2. B. O'Regan and M. Grätzel, *Nature*, **353**, 737 (1991).
3. T.-C. Wei, S.-P. Feng, Y.-H. Chang, S.-J. Cherng, Y.-J. Lin, C.-M. Chen, and H.-H. Chen, *Int. J. Electrochem. Sci.*, **7**, 11904 (2012).
4. J.-L. Lan, C.-C. Wan, T.-C. Wei, W.-C. Hsu, C. Peng, Y.-H. Chang, and C.-M. Chen, *Int. J. Electrochem. Sci.*, **6**, 1230 (2011).
5. A. Yella, H.-W. Lee, H. N. Tsao, C. Yi, A. K. Chandiran, M. K. Nazeeruddin, E. W.-G. Diau, C.-Y. Yeh, S. M. Zakeeruddin, and M. Grätzel, *Science*, **334**, 629 (2011).
6. T. Yamaguchi, N. Tobe, D. Matsumoto, T. Nagai, and H. Arakawa, *Sol. Energy Mater. Sol. Cells*, **94**, 812 (2010).
7. J. H. Park, Y. Jun, H.-G. Yun, S.-Y. Lee, and M. G. Kang, *J. Electrochem. Soc.*, **155**, F145 (2008).
8. S. Ito, N.-L. C. Ha, G. Rothenberger, P. Liska, P. Comte, S. M. Zakeeruddin, P. Pechy, M. K. Nazeeruddin, and M. Grätzel, *Chem. Commun.*, 4004 (2006).
9. T.-Y. Tsai, C.-M. Chen, S.-J. Cherng, and S.-Y. Suen, *Prog. Photovolt: Res. Appl.*, **21**, 226 (2013).
10. M. G. Kang, N.-G. Park, K. S. Ryu, S. H. Chang, and K.-J. Kim, *Chem. Lett.*, **34**, 804 (2005).
11. Y. Jun and M. G. Kang, *J. Electrochem. Soc.*, **154**, B68 (2007).
12. Y. Jun, J. Kim, and M. G. Kang, *Sol. Energy Mater. Sol. Cells*, **91**, 779 (2007).

Downloaded on 2013-11-18 to IP 140.120.136.205 address. Redistribution subject to ECS license or copyright; see ecsdl.org/site/terms_use

13. T. Ma, X. Fang, M. Akiyama, K. Inoue, H. Noma, and E. Abe, *J. Electroanal. Chem.*, **574**, 77 (2004).
14. C.-M. Chen, C.-H. Chen, and T.-C. Wei, *Electrochim. Acta*, **55**, 1687 (2010).
15. S.-J. Cherng, C.-M. Chen, W.-P. Dow, C.-H. Lin, and S.-W. Chen, *Electrochem. Solid-State Lett.*, **14**, P13 (2011).
16. Y.-T. Huang, S.-P. Feng, and C.-M. Chen, *Electrochim. Acta*, **99**, 230 (2013).
17. T. N. Murakami, Y. Kijitori, N. Kawashima, and T. Miyasaka, *J. Photochem. Photobiol. A: Chem.*, **164**, 187 (2004).
18. T. Watanabe, H. Hayashi, and H. Imai, *Sol. Energy Mater. Sol. Cells*, **90**, 640 (2006).
19. D. Gutiérrez-Tauste, I. Zumeta, E. Vigil, M. A. Hernández-Fenollosa, X. Domènech, and J. A. Ayllón, *J. Photochem. Photobiol. A: Chem.*, **175**, 165 (2005).
20. Y. Kijitori, M. Ikegami, and T. Miyasaka, *Chem. Lett.*, **36**, 190 (2007).
21. H. Pan, S. H. Ko, N. Misra, and C. P. Grigoropoulos, *Appl. Phys. Lett.*, **94**, 071117 (2009).
22. X. Li, H. Lin, J. Li, N. Wang, C. Lin, and L. Zhang, *J. Photochem. Photobiol. A: Chem.*, **195**, 247 (2008).
23. D. Zhang, T. Yoshida, K. Furuta, and H. Minoura, *J. Photochem. Photobiol. A: Chem.*, **164**, 159 (2004).
24. M. Ikegami, K. Miyoshi, T. Miyasaka, K. Teshima, T. C. Wei, C. C. Wan, and Y. Y. Wang, *Appl. Phys. Lett.*, **90**, 153122 (2007).
25. W.-P. Dow, G.-L. Liao, S.-E. Huang, and S.-W. Chen, *J. Mater. Chem.*, **20**, 3600 (2010).
26. K. Akamatsu, H. Shinkai, S. Ikeda, S. Adachi, H. Nawafune, and S. Tomita, *J. Am. Chem. Soc.*, **127**, 7980 (2005).
27. Y.-S. Hsiao, W.-T. Whang, S.-C. Wu, and K.-R. Chuang, *Thin Solid Films*, **516**, 4258 (2008).
28. W. Liu, L. Hu, S. Dai, L. Guo, N. Jiang, and D. Kou, *Electrochim. Acta*, **55**, 2338 (2010).

Downloaded on 2013-11-18 to IP **140.120.136.205** address. Redistribution subject to ECS license or copyright; see **ecsdl.org/site/terms_use**